

Short Communication

## Effect of Microstructures on Surface Properties of Electrochemical Machining of Ti-5.6Al-2Zr-4.8Sn-1Mo-0.35Si-0.7Nd Alloys

Yaowu Zhou<sup>1</sup>, Zhengyang Xu<sup>1,\*</sup>, Xuezhen Chen<sup>2</sup>, Yu Tang<sup>1</sup>

<sup>1</sup> College of Mechanical and Electrical Engineering, Nanjing University of Aeronautics and Astronautics, Nanjing 210016, China

<sup>2</sup> NC Processing Plant, AVIC Chengdu Aircraft Industrial(Group) CO.,LTD.,Chengdu,610092,China

\*E-mail: [xuzhy@nuaa.edu.cn](mailto:xuzhy@nuaa.edu.cn)

Received: 10 September 2019 / Accepted: 21 November 2019 / Published: 31 December 2019

Electrochemical machining (ECM) has been widely used to process high-temperature titanium alloys, however, few studies have investigated the ECM of Ti-5.6Al-2Zr-4.8Sn-1Mo-0.35Si-0.7Nd (Ti60). This study examined the differences in the microstructures of the Ti60 forged with two different methods, focusing on the influences of the material microstructures on the surface morphology produced by ECM. The  $\beta$ -forged Ti60 reveal a small and staggered grains and a more uniform distribution of the  $\alpha$  and  $\beta$  phases, and the surface morphology produced by ECM is better than that of the conventional forged Ti60. ECM experiments of the Ti60 were also carried out to analyze the influence of the current density on the surface roughness. The results show that the surface roughness of the Ti60 produced by ECM is adversely affected when the current density is either small or increases considerably. The best surface quality of the two kinds of Ti60 is obtained when the current density is about 50 A/cm<sup>2</sup>.

**Keywords:** Electrochemical machining, Ti-5.6Al-2Zr-4.8Sn-1Mo-0.35Si-0.7Nd, Microstructure, Current density

### NOMENCLATURE

ECM = Electrochemical Machining

## 1. INTRODUCTION

In order to meet the requirements for lighter aero engines with higher thermal efficiency, “difficult-to-machine” materials such as titanium and its alloys are often used to manufacture the components of these engines. Near- $\alpha$  titanium alloys are the most important type of structural materials used for compressor components, such as blisks of advanced gas turbine engines [1]. The main advantage of these alloys is their low density and good high-temperature mechanical properties. Ti-5.6Al-4.8Sn-

2Zr–1Mo–0.35Si–0.7Nd is a near- $\alpha$  titanium alloy with an optimized chemistry which makes it possible to operate at service temperatures up to 600°C [2-4]. However, the traditional method for processing this material is not desirable due to low processing efficiency, poor precision, and severe tool wear. The surface integrity of the resulting component also tends to be poor because of thermo-mechanical alteration or damage to the rim zones [5-9]. Therefore, an effective use of Ti60 requires unconventional manufacturing technologies.

Electrochemical machining (ECM), a process whereby material is removed by electrochemical dissolution of a workpiece, is a promising method that offers considerable advantages for processing the difficult-to-cut Ti60, including the absence of mechanical influences on a machining surface, absence of tool wear, high processing efficiency. In addition, with ECM it is possible to achieve a finished surface without white layers or heat-affected zones. Thus, the ECM method has received increasing attention from researchers [5].

The ECM of titanium alloys has attracted much attention. The electrochemical dissolution of three titanium materials in three solutions with different pH was studied by Baehre [10]. He found that the increase in titanium in the material hindered electrochemical dissolution, and that halogen-containing electrolytes were preferred for processing titanium alloys. He [11] studied the electrochemical reactions of Ti6Al4V in the NaNO<sub>3</sub> solution, NaCl solution and mixed solution, finding the phenomenon of electrochemical polarization under low current density, mechanism of electrochemical dissolution, and surface morphology under high current density. This study also showed that the mixed electrolyte can effectively reduce pit-like dissolution and pitting corrosion and thus improve the surface quality. In addition, the experiment of side-flow electrochemical machining was carried out, showing that with the increase of feed speed, the average machining current increased linearly, and that the surface roughness decreased rapidly [12]. Mount [13] performed a theoretical analysis of the chronoamperometric transients in ECM and the characterization of titanium 6/4 and Inconel 718 alloys. Zhu [14] simulated several ECM flow fields of a nickel-based and titanium-based diffuser, and verified by experiments that the flow pattern of the electrolyte from the leading edge to trailing edge was most suitable for ECM of a diffuser with long and thin blades. Lu [15] employed jet-electrochemical micromachining to produce micro-hole patterns in titanium specimens. Van Camp [16] processed titanium alloys through mechanical electrochemical milling, which improved the processing efficiency and processing stability of titanium alloys. Anasane [17] carried out micro-machining of titanium alloy through electrochemical micromachining, and studied the influence of various EMM process parameters, such as machining voltage, pulse frequency and micro-knife feed rate, on the machining accuracy of micro-grooves. Tsai [18] presented a technology of electrochemical abrasive jet machining to remove the oxide film on the surface of titanium alloys via the impact of abrasive on the electrolytic surface of titanium alloys, thus improving the efficiency of ECM.

Although many researchers have focused on the ECM of different titanium alloys, there has been little research on the ECM of Ti60. In this paper, the influences of the material microstructures of Ti60 on its surface morphology formed by ECM are discussed, and analyzed the influence of the current density on the surface roughness through ECM experiments of Ti60.

## 2. MATERIALS AND METHODS

### 2.1 Workpiece Material

The workpieces were fabricated with two variations of Ti60. One was produced by the traditional forging method with the forging temperature lower than the phase transition point of titanium alloys, and the other was fabricated by a  $\beta$ -forging method with the forging temperature higher than the phase transition point of titanium alloys. Fig. 1(a) and Fig. 1(b) show the microstructures of the Ti60 produced by the traditional forging and the Ti60 produced by the  $\beta$ -forging method respectively. Fig.1(a) shows that the bulk spherical grains are primary  $\alpha$  phases, and the rest  $\beta$  transition tissues made up of secondary  $\alpha$  lamellae and interlamellar residual tissue  $\beta$  phases. The primary  $\alpha$  phases are separated by the  $\beta$  transition tissues. On the other hand, the  $\beta$ -forged Ti60 is deformed near the  $(\alpha + \beta)/\beta$  phase transition point or in the  $\beta$ -phase region. When the deformation increases from 50% to 80%, the existing  $\beta$  grains and the boundaries of the equiaxed  $\alpha$  grains are broken. After the material is cooled to room temperature, the size of the  $\alpha$  cluster is greatly reduced and the lamellae  $\alpha$  phases with the retained  $\beta$  phases are formed. That is, a basket-weave microstructure is formed.

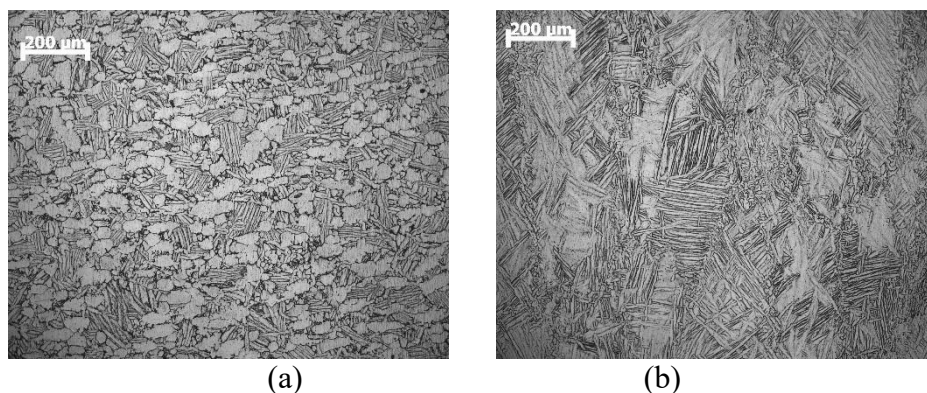


**Figure 1.** Microstructures of Ti60 materials. (a) Ti60 formed with conventional forging method and (b) Ti60 formed with  $\beta$  forging method.

### 2.2 ECM Experimental System

The ECM experimental system is rather complex, including a single-axis ECM machine tool, control system, electrolyte circulation and filter system, pulse power supply, cathode, fixture for clamping the cathode, and the workpiece. During the ECM process, the cathode is clamped by the fixture while the workpiece, which acts as the anode, is fed towards the cathode. A small inter-electrode gap is maintained between the workpiece and the cathode, and the electrolyte is pumped into the gap at high pressure to remove the electrochemical products. To produce a better surface texture or a high-precision workpiece, the machining process parameters are kept stable, such as the electrolyte concentration, electrolyte flow rate and pressure, temperature, power voltage, and feed velocity. Membrane filtration capable of filtering down to 0.5  $\mu\text{m}$  and a frame filter are used to ensure the purity of the electrolyte. The electrolyte temperature can be maintained by a heat exchanger with an accuracy of  $\pm 0.1^\circ\text{C}$ . A schematic

of the electrochemical machining device is shown in Fig. 2(a). The workpiece is 10 mm × 10 mm × 20 mm square stock, as shown in Fig. 2(b). The surfaces machined by the ECM are shown in Fig. 2(c).

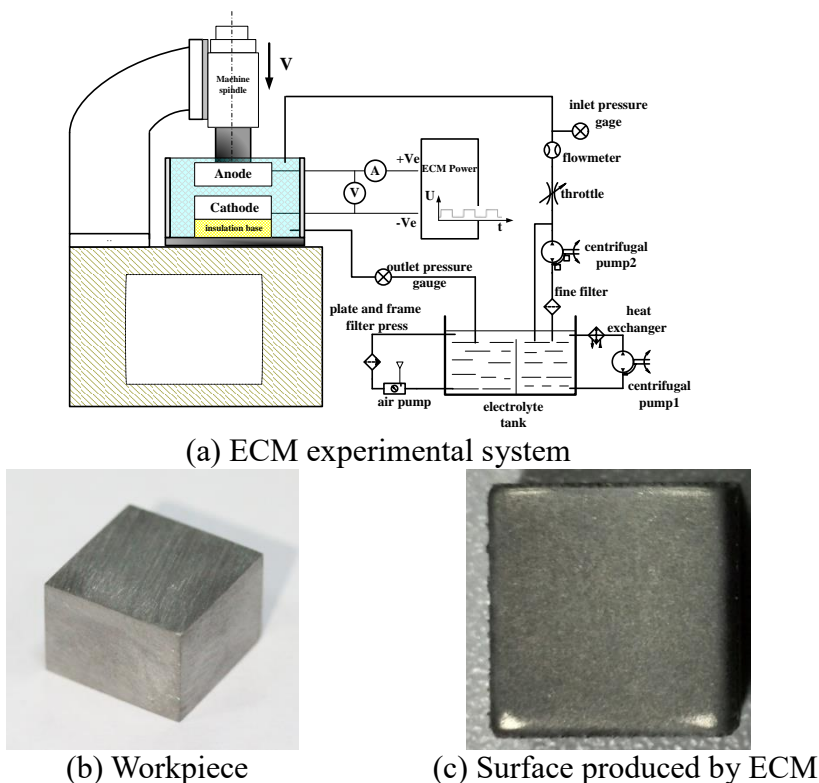


Figure 2. ECM experimental system and workpiece

2.3 ECM Experimental Parameters

Table 1. ECM experimental parameters

Item	Value
Workpiece material	Ti60, forged in two different ways
Cathode material	1Cr18Ni9Ti stainless steel
Electrolyte	NaCl (130.3 g/L)
Voltage	30 V
Power frequency	1.0 KHz
Duty cycle	0.5
Inlet pressure	0.5 MPa
Temperature of electrolyte	40 ± 0.1°C
Initial gap	0.5 mm
Feed rate	0.5 - 1.5 mm/min

The ECM experiments of the Ti60 were performed on the experimental system that we had developed, with the machining time being five minutes. The main experimental parameters are listed in Table 1. The workpieces were fabricated from the two types of Ti60 forged by the traditional and β-

forging methods. The tool electrodes are made of stainless steel. We used sodium chloride because the halogen-containing electrolytes are preferred for processing titanium alloys [10]. In order to make the titanium alloy stable for machining and produce a better surface finish on the titanium, the parameters of the voltage and temperature were set to higher values than those used for nickel-based alloys. A pulse power supply was used to improve machining stability and quality, and different feed rates were used to attain different machining current densities during the ECM process.

### 3. RESULTS AND DISCUSSION

Fig. 3 shows the microstructures of the Ti60 formed by ECM. Figs. 3(a) and (b) are the microstructures of the conventionally forged Ti60 with different ECM current densities. Figs. 3(c) and (d) are the microstructures of the  $\beta$ -forged Ti60 with different ECM current densities. The ECM-machined microstructures conform to the original morphologies of the Ti60 formed with the two different forging methods, as shown in Fig. 1. The  $\beta$  transition tissues are prominent and the  $\alpha$  phase is concave, which is caused by the difference in the dissolution rate between the two tissues. For Ti60 alloys, or

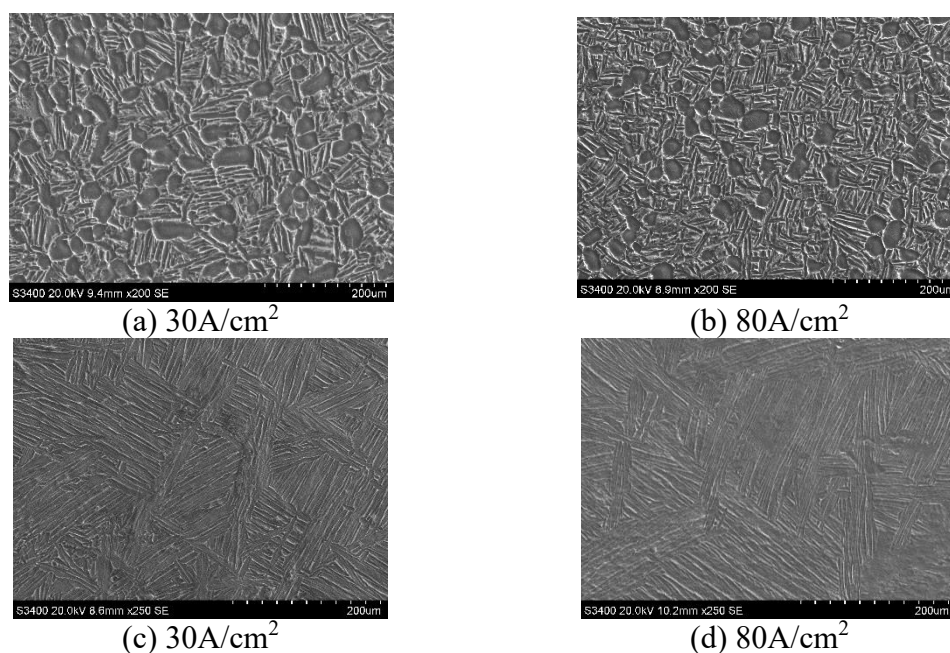


**Figure 3.** ECM-formed microstructure morphologies of Ti60

Ti-5.6Al-2Zr-4.8Sn-1Mo-0.35Si-0.7Nd, the aluminum (Al) acts as the  $\alpha$  stabilizing element and tends to concentrate in the  $\alpha$  phase. Molybdenum (Mo) and silicon (Si) are the  $\beta$ -stabilizing elements which tend to locate in the  $\beta$  transition tissue. Neodymium (Nd) is rare element, mainly distributed in the gap between the  $\alpha$  and  $\beta$  phases, to reduce the activation energy of grains and prevent excessive growth of grains, without affecting the electrochemical properties between the tissues. Zirconium (Zr) and tin (Sn) are neutral elements which have the same distribution degree in the  $\alpha$  and  $\beta$  phases. Al has

the lowest electrode potential and a greater electrochemical equivalent, thus it will be dissolved preferentially based on the electrochemistry theory. Mo and Si have a higher electrode potential and lower electrochemical equivalent, thus more difficult to machine electrochemically than Al.

Fig. 4 shows the 3D morphologies of the conventionally forged Ti60 with different ECM current densities. When the current density is 30 A/cm<sup>2</sup>, the workpiece surface is smooth, with a surface roughness Ra of 1.239 μm. When current density is increased to 80 A/cm<sup>2</sup>, an undulating surface occurs with a surface roughness Ra of more than 2.093 μm. This is because the concave α phase becomes more obvious with the increase of current density, which will deteriorate the surface roughness.

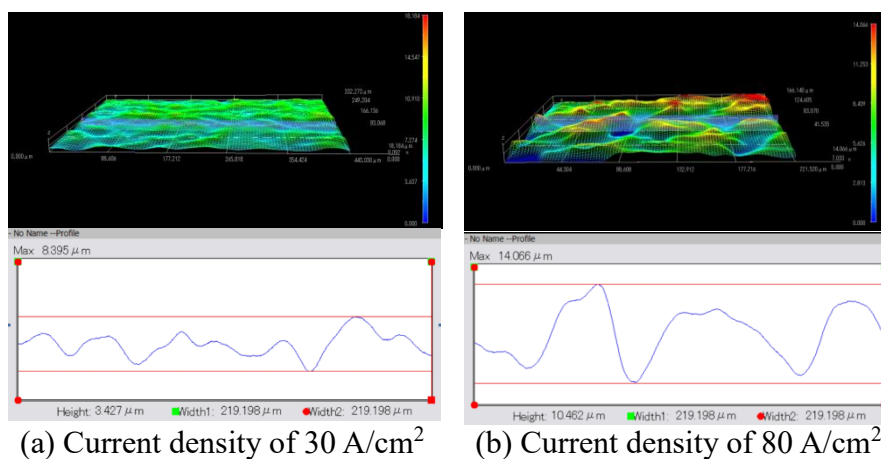


**Figure 4.** 3D morphologies of conventionally forged Ti60 with different ECM current densities

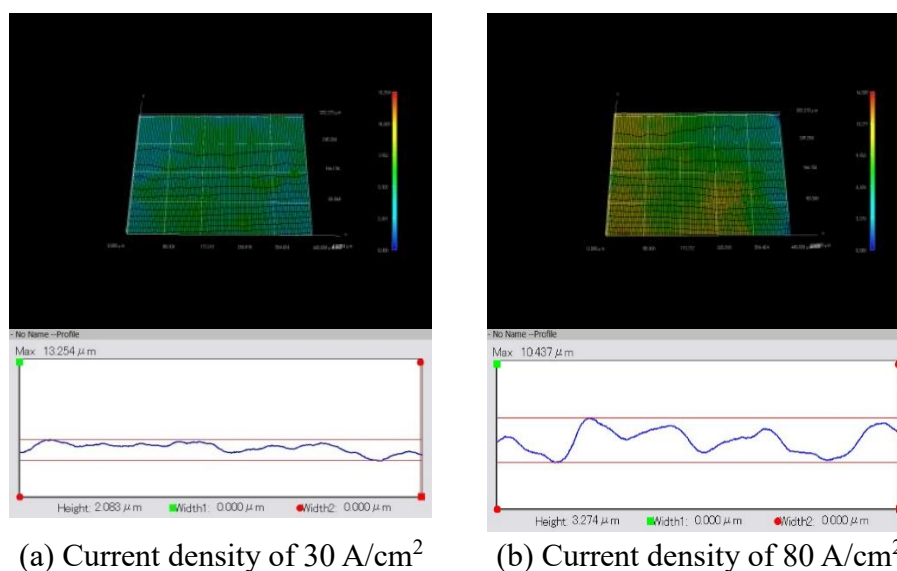


**Figure 5.** 3D morphologies of β-forged Ti60 with different ECM current densities

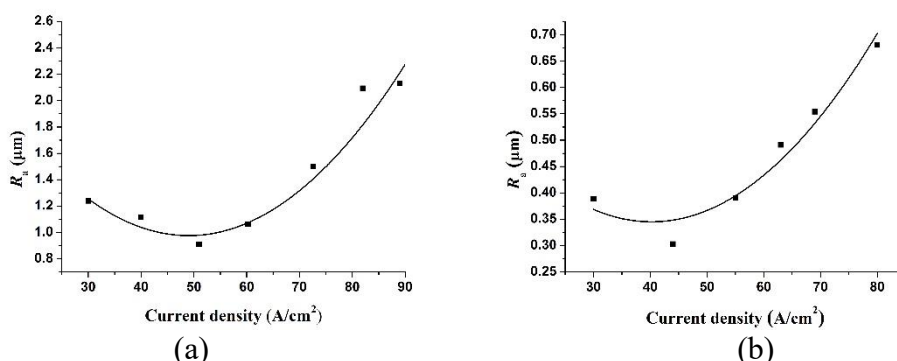
Fig. 5 shows the 3D morphologies of the β-forged Ti60 with different ECM current densities. When the current density is 30 A/cm<sup>2</sup>, the β-forged Ti60 surface is very smooth with the surface roughness Ra being only 0.389 μm. When the current density is increased to 80 A/cm<sup>2</sup>, the workpiece

surface remains smooth, but Ra increases slightly to 0.681  $\mu\text{m}$ . This is due to the  $\beta$  tissues vary little with the increasement of current density, therefore, the surface roughness of workpiece is relatively smooth.

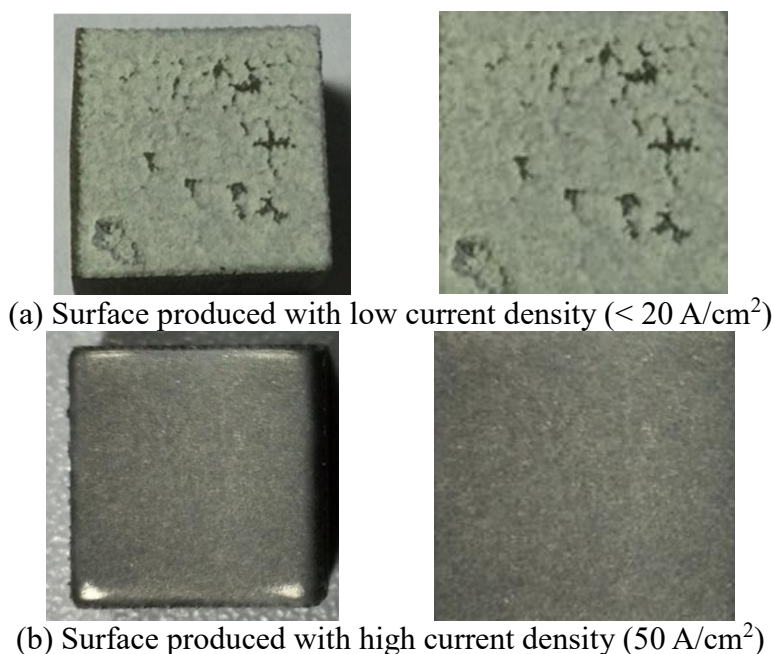
The electrochemically machined surface of the  $\beta$ -forged Ti60 is much better than that of the conventionally forged Ti60. The main reason for this is that, with the  $\beta$ -forged method, the titanium forging deformation is above the phase transition point, resulting in the fracture of the original  $\alpha$  phase and  $\beta$  phase grains. After being fractured, the  $\alpha$  grains become shorter and staggered without a large equiaxed  $\alpha$  phase. Therefore, the  $\beta$  phase is more uniformly distributed among the  $\alpha$  phase, the grains are denser, and the distributions of different elements are more uniform, leading to a better surface and roughness. The analysis of the prominent  $\beta$  transition tissues and the concave  $\alpha$  phase in Section 2.1 Workpiece material shows that the  $\beta$ -forged Ti60 is more uniformly dissolved. Compared with the  $\beta$ -forged Ti60, the conventional forged Ti60 reveals more apparent changes in the surface, resulting in a higher roughness.

Fig. 4 and Fig. 5 show that the machining surface quality of the Ti60 worsens as the current density of the ECM is increased. To increase the reliability of this research, a large number of current density experiments were conducted for the conventionally forged Ti60 and the  $\beta$ -forged Ti60. The experimental results are presented in Fig 6, showing that the surface roughness of the workpiece decreases first and then increases with the increase of the current density. When the current density is low, the passivation film is more serious, resulting in difficult to dissolution and poor roughness, as shown in Fig. 7(a). When the current density increases, the dissolution rate between different tissues changes, resulting in a poor roughness. Therefore, the best surface quality is obtained when the current density is about 50  $\text{A}/\text{cm}^2$ , as shown in Fig. 7(b).

The conventionally forged Ti60 and the  $\beta$ -forged Ti60 have same elements, the roughness change trend of the processed surface is consistent in different current density.



**Figure 6.** Relationship between surface roughness and current density. (a) Conventionally forged Ti60 and (b)  $\beta$ -forged Ti60.



**Figure 7.** Surfaces produced by ECM with different current densities

The hard to machine titanium alloys play an important role in aeronautics and astronautics fields. Hood [19] reported that by using small diameter end milling tools to improve integrity of  $\gamma$ -TiAl intermetallic alloy. Klocke [20] has done the experiments of feed rate as a function of current density for an ECM sinking operation with a cylindrical tool electrode, and the surface properties of titanium- and nickel-based alloys were examined in terms of SEM and EDX analysis of the rim zone. Weinmann [21] has investigated the dissolution behavior of Ti90Al6V4 alloy and self-produced Ti60Al40 alloy in aqueous electrolytes, and the experimental results showed that an increase of chloride ions in the electrolyte and higher titanium content of the alloy could facilitate the dissolution process in ECM. In this paper, the influence of  $\alpha$  and  $\beta$  phases on the surface roughness of Ti60 has been investigated firstly with different current density.

#### 4. CONCLUSION

(1) The influence of the different material microstructures of Ti60 on the surface morphology produced by electrochemical machining was investigated in this study. Compared to the conventionally forged Ti60, the  $\beta$ -forged Ti60 can more easily attain a better surface roughness. The main reason for this finding is that the  $\beta$  grains and equiaxed  $\alpha$  grains are broken by the  $\beta$  forging method. The  $\beta$ -forged titanium alloy Ti60 exhibits a basket weave microstructure, in which the grains become shorter and narrower and the distribution of the elements is more uniform. Different elements in different tissues lead to differences in dissolution rate.

(2) The ECM experiments of Ti60 were carried out to analyze the influence of current density on surface roughness. When the current density is low, the electrochemical dissolution is found to be abnormal and a large amounts of stray current corrosion on the surface occurs. When the current density is greatly increased, the dissolution velocity differences of the metal elements also increase rapidly,

resulting in a poorly machined surface. Thus, the Ti60 surface roughness produced by ECM, deteriorates when the current density is either small or increases significantly. The best surface quality is obtained when the current density is about 50 A/cm<sup>2</sup>.

#### ACKNOWLEDGEMENTS

This research was sponsored by the National Natural Science Foundation of China (9196204), the Outstanding Youth Foundation of Jiangsu province of China (BK20170031) and the Fundamental Research Funds for the Central Universities (NE2014104).

#### References

1. S. Z. Zhang, M. M. Li, L. Q. Chen, *Mater. Sci. Eng. A.*, 564 (2013) 317.
2. Y. Niu, H.L. Hou, M.Q. Li, Z.Q. Li, *Mater. Sci. Eng. A.*, 492 (2008) 24.
3. S. Z. Zhang, H. Z. Xu, G. P. Li, Y.Y. Liu, R. Yang, *Mater. Sci. Eng. A.*, 408 (2005) 290.
4. M. Q. Li, H. S. Pan, Y. Y. Lin, J. Luo, *J. Mater. Process. Technol.*, 183 (2007) 71.
5. A. D. Davydov, T. B. Kabanova, V. M. Volgin, *Russ. J. Electrochem.*, 53 (2017) 941.
6. A. Pramanik, *Int. J. Adv. Manuf. Technol.*, 70 (2014) 919.
7. I. S. Jawahir, E. Brinksmeier, R. M'Saoubi, D. K. Aspinwall, J. C. Outeiro, D. Meyerb, D. Umbrello, A. D. Jayala, *CIRP Ann. Manuf. Technol.*, 60 (2011) 603.
8. S. L. Soo, R. Hood, D. K. Aspinwall, W.E. Voice, C. Sage, *CIRP Ann. Manuf. Technol.*, 60 (2011) 89.
9. D. Zhu, D. Zhu, Z. Y. Xu, L.S. Zhou, *Chinese J. Aeronaut.*, 26 (2013) 1064.
10. D. Baehre, A. Ernst, K. Weißhaar, H. Natter, M. Stolpe, R. Busch, *Procedia Cirp*, 42 (2016) 137.
11. Y.F. He, H.X. Xiao, W.M. Gan, Q. Yu, F.H. Y, *Procedia Cirp.*, 68 (2018) 751.
12. Y.F. He, J.S. Zhao, H.X. Xiao, W.Z. Lu, W.M. Gan, F.H. Yin, Z.W. Yang, *Int. J. Electrochem. Sci.*, 13 (2018) 5736.
13. A. R. Mount, K. L. Eley, D. Clifton, *J. Appl. Electrochem.*, 30 (2000) 447.
14. D. Zhu, Z.Z. Gu, T.Y. Xue, D. Zhu, *Procedia Cirp.*, 42 (2016) 121.
15. X. Lu and Y. Leng, *J. Mater. Process. Technol.*, 169 (2005) 173.
16. D.V. Camp, J. Qian, J. Vleugels, B. Lauwers, *Cirp Annals.*, 67 (2018) 217.
17. S.S. Anasane and B. Bhattacharyya. *J. Manuf. Process.*, 28 (2017) 285.
18. F. C. Tsai, Y. L. Lee, J. C. Yeh, *Ind. Lubr. Tribol.*, 70 (2018) 1545.
19. R. Hood, D.K. Aspinwall, S.L. Soo, A.L. Mantle, D. Novovic. *Cirp Annals.*, 63 (2014) 53.
20. F. Klocke, M. Zeis, A. Klink, D. Veselovac. *Procedia Cirp.*, 6 (2013) 368.
21. M. Weinmann, M. Stolpe, O. Weber, R. Busch H. Natter. *J. Solid. State. Electr.*, 19 (2015) 485.

© 2020 The Authors. Published by ESG ([www.electrochemsci.org](http://www.electrochemsci.org)). This article is an open access article distributed under the terms and conditions of the Creative Commons Attribution license (<http://creativecommons.org/licenses/by/4.0/>).